

***Ab initio* simulation of high-pressure phases of GaAs**

Murat Durandurdu and D. A. Drabold

Department of Physics and Astronomy, Condensed Matter and Surface Science Program, Ohio University, Athens, Ohio 45701

(Received 12 December 2001; published 31 July 2002)

The pressure-induced phase transition in GaAs is studied using an *ab initio* constant-pressure relaxation simulation. GaAs undergoes a first-order phase transition to *Cmcm* at 54 GPa. Upon further increase of pressure a gradual phase change to *Imm2* structure is seen at 57 GPa, which confirms an earlier experiment and clears some doubts about the existence and identity of *Imm2*. The transition pressures are also calculated from the Gibbs free energy, and it is found that the structural phase change occurs at 23.5 GPa for *Cmcm* and at 24 GPa for *Imm2*. The transformation path from *Cmcm* and *Imm2* proceeds through sliding of some *Cmcm* planes and relatively large sliding yields a transition from *Imm2* to simple hexagonal structure. We find that *Cmcm* and *Imm2* phases are semimetals.

DOI: 10.1103/PhysRevB.66.045209

PACS number(s): 64.70.Kb, 71.30.+h, 61.50.Ks

I. INTRODUCTION

Numerous experimental and theoretical investigations have successfully identified high-pressure phases of semiconductors. In the case of GaAs, the high-pressure phases are the subject of many speculations. Recently GaAs-II has been determined to have *Cmcm* structure. However, the identity of GaAs-III remains unsolved. In this study, we perform a first-principles calculation to elucidate the high-pressure phases of GaAs and a possible transition path between GaAs-II and GaAs-III.

An earlier x-ray-diffraction study¹ has reported on several high-pressure phases of GaAs at room temperature; GaAs-I (zinc blende) \rightarrow GaAs-II \rightarrow GaAs-III (*Imm2*) \rightarrow GaAs-IV (simple hexagonal) at about 17, 24, and 60–80 GPa, respectively. The study assigned GaAs-II as an orthorhombic (*Pmm2*) structure. Motivated by experiment, Zhang and Cohen² performed a first-principles calculation and found that this structure is thermodynamically favored over the rocksalt structure. However, a recent experiment using the angle-dispersive technique³ has reported that the structure of GaAs-II is *Cmcm*, which is observed in ZnTe (Ref. 4) and InSb.⁵ In addition, the experiment has shown that there is no phase transition to GaAs-III above 24 GPa. Mujica and Needs⁶ performed a first-principles calculation and found that *Cmcm* structure is more stable than *Pmm2* for GaAs.

In contrast to Si and Ge, the GaAs-II phase transforms back to zinc-blende (ZB) structure upon decompression. McMahon and Nelmes⁷ observed a new hexagonal phase, four-fold coordinated *Cinnabar*, between *Cmcm* and ZB phase on the pressure release. They also reported that *Cinnabar* phase persists with applied pressure before transforming to *Cmcm* at about 15 GPa and on further pressure release it transforms to ZB phase near 4 GPa. However, there is no evidence of a transformation from ZB to *Cinnabar* on pressure increase at room temperature. First-principles calculation^{8,9} have found that *Cinnabar* phase is thermodynamically unstable.

First-principles calculations using thermodynamic criterion of equal free energies have successfully explained pressure-induced phase transitions. However, the methods can be only applied to known structures. In principle, first-

principles dynamical simulations are preferable, which may provide detailed information about transition paths and electronic structure of phases for each applied pressure. Unfortunately the predicted transition pressures are commonly larger than experimental and theoretical (from the free-energy calculations) values. The large value of the metastable transition pressure from the dynamical simulations can be attributed to an intrinsic activation barrier, and hence the simulation cell is superpressurized in analogy to isobaric superheating in simulations.^{10,11}

In this paper, we perform a partial study of the GaAs phase diagram by simulating the response of GaAs to pressure. In our calculation, we (1) directly simulate pressure-induced phase transitions by dynamical simulation from Parrinello–Rahman method,¹² and (2) use the structure of Gibbs free energy at zero temperature ($G = E_{tot} + PV$) to accurately estimate transition pressures that are overestimated in the dynamical simulations (Parrinello–Rahman method) because of kinetics. Potentially significant features of the transitions are neglected here, including entropic contributions from lattice vibrations. The dynamical simulations successfully identify the high-pressure phases of GaAs with overestimated transition pressures. Nevertheless, the simulations eliminate doubts about the identity of both phases. The predicted transition pressure from the Gibbs free-energy calculations is 23.5 GPa for *Cmcm* and 24 GPa for *Imm2*, which are comparable to the experimental results. The transformation from *Cmcm* to *Imm2* is associated with the sliding of some planes of *Cmcm* structure. Both high-pressure phases of GaAs are semimetallic.

II. METHODOLOGY

The simulation reported here is carried out in a 216-atom model of GaAs that is initially arranged in ZB structure at initial lattice parameter $a_0 = 5.658$ Å. We use a local-orbital quantum molecular dynamic method.¹³ The essential approximations are (1) nonlocal, norm-conserving pseudopotentials, (2) slightly excited local-orbital basis set of four orbitals per site, and (3) the Harris functional implementation of density-functional theory in the local-density approximation. This method has been successfully applied to predict

expanded volume phases of GaAs,¹⁴ and pressure-induced phase transition in crystalline silicon (a diamond to simple hexagonal), in amorphous silicon (first-order amorphous to amorphous),¹⁵ and a continuous amorphous to amorphous phase transformation in GeSe₂.¹⁶ For each pressure, slow dynamical quenching starting at 1400 K is performed to fully relax the ZB structure to zero temperature. For dynamical approach, pressure is applied via the method of Parrinello and Rahman,¹² which enables the simulation cell to change volume and shape. The number of steps was selected to ensure that the system was completely relaxed (according to the criterion that the maximum force was smaller than 0.01 eV/Å). All the calculations used solely the Γ point to sample the Brillouin zone, which is reasonable for a cell with 216 atoms. A fictitious cell mass of 15×10^3 amu was found to be suitable for these simulations.

III. RESULTS AND DISCUSSION

A. Parrinello–Rahman simulation

In order to understand the mechanism of the semiconductor to metal transition, we first plot the pressure dependence of the relative volume from the dynamical approach in Fig. 1. The volume changes smoothly up to 39 GPa. At this pressure, an abrupt decline of the volume is seen. In the pressure range 39–54 GPa, the volume decreases gradually and at 54 GPa another small change of the volume relative to the first one is obtained. Up to 65 GPa no sharp modification of volume is seen.

In tetrahedrally bonded materials, initial compression causes a reduction of bond lengths and change of bond angles. The structural properties of GaAs under pressure are given in Table I. The average bond length and bond angle decrease smoothly up to 39 GPa. At this pressure, a slight increase of the average bond length is seen while the average bond angle and especially the width of the bond angle distribution changes significantly without modification of coordination indicating that a transition to a distorted structure takes place (Fig. 3). This result is consistent with the experiment¹⁷ that has reported that GaAs presents “crystalline disorder” before it transforms into GaAs-II. At ambient temperature, the phase transition in GaAs tends to be sluggish and diffraction patterns of the high-pressure phases characterized by broad peaks indicative of strain and disorder.¹⁸ In the pressure range 39–54 GPa, the average bond angle and the width of the bond angle distribution exhibit a significant modification, implying more distorted phases. The structures in the pressure range 39–54 GPa do not have partial sixfold coordination as reported in the experiment,¹⁷ which is probably due to the use of a perfect crystalline structure with periodic boundary conditions. In a perfect crystal, the compression is uniformly distributed and nucleation centers for phase transitions do not exist, which may hinder a partial coordination change and favor a global coordination modification. When defects are introduced a transition nucleates at defects, which is seen in the previous study of amorphous materials under pressure, and in simulation of the solid to liquid phase transition of silicon.¹⁹

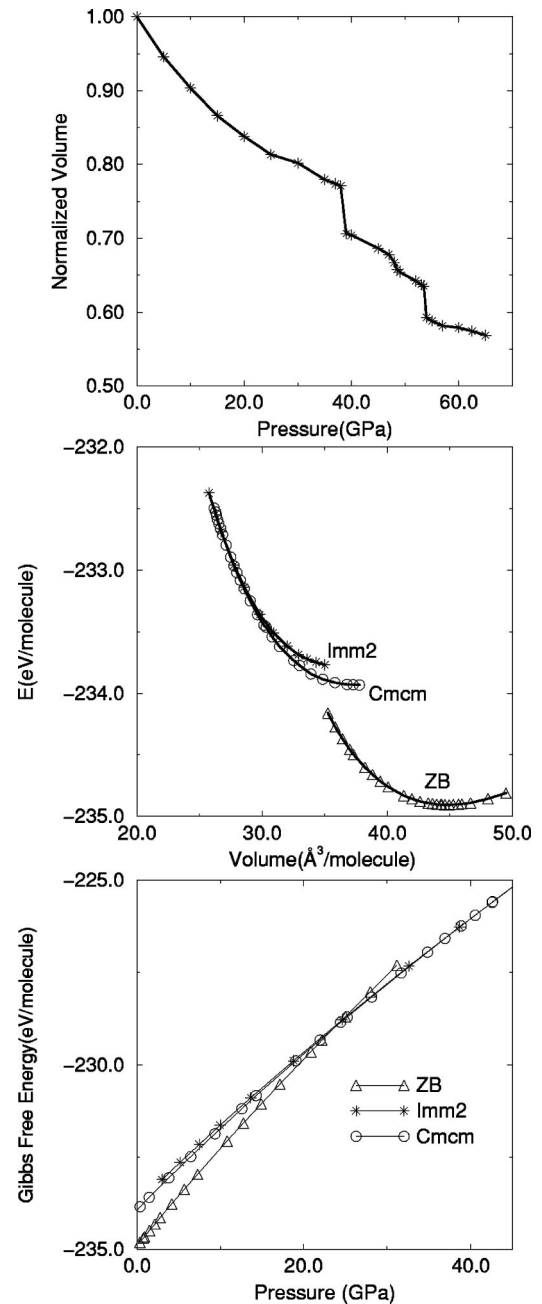


FIG. 1. (a) The normalized volume to the zero-pressure measured volume. (b) The energy E in eV per molecule versus the volume per molecule for ZB and the $Cmcm$ and $Imm2$ phase. (c) The Gibbs free energy of ZB and $Cmcm$ and $Imm2$ structures.

The second abrupt change of the structural parameters is seen at 54 GPa. The average bond length increases and the coordination changes from fourfold to sixfold. All bonds are heteropolar. The bond angle distribution function of the obtained structure at 54 GPa is given in Fig. 2. The structure presents several peaks at about 70° , 82° , 90° , 98° , 109.6° (close to the ideal tetrahedral angle), 140° , 162° , and 177° . The structure at 54 GPa is depicted in Fig. 3. The structure is a zigzag stacking of slightly distorted NaCl-like planes. The phase is only compatible with $Cmcm$ structure of GaAs, which can be related to NaCl phase by shearing of alternate

TABLE I. Structural properties of GaAs under pressure, average bond length (ABL), average bond angle (ABA), width of bond angle distribution (WBAD), and average coordination number (ACN).

Pressure (GPa)	35	39	53.5	54	57
ABL (Å)	2.241	2.265	2.273	2.41	2.405
ABA (degree)	109.40	106.76	104.415	103.995	104.84
WBAD (degree)	2.58	16.06	20.964	30.74	30.65
ACN	4.0	4.0	4.0	6.0	6.0

(010) planes and a puckering of [100] rows. Mujica and Needs⁶ have reported that the NaCl phase is unstable to such shearing of (010) planes, which is the driving force leading to a *Cmcm* structure, while puckering and cell shape distortions are consequences of the shearing. *Cmcm* is a usual structure seen in II-VI and III-V semiconductors.³ We find $b/a \sim 0.983$ and $c/a \sim 1.046$, which are in good agreement with the experimental values of $b/a = 0.973$ and $c/a = 1.055$,¹ and the theoretical results of $b/a = 0.953$ and $c/a = 1.049$.⁶ The transition volume of the *Cmcm* in the constant-pressure relaxation simulation is 26.5 \AA^3 per molecule volume. However, it is found to be 30.447 \AA^3 in the thermodynamic criterion of the Gibbs free-energy calculation (see below), which is in a good agreement with an accurate self-consistent calculation result of 31.538 \AA^3 per molecule volume of *Cmcm* phase.⁶

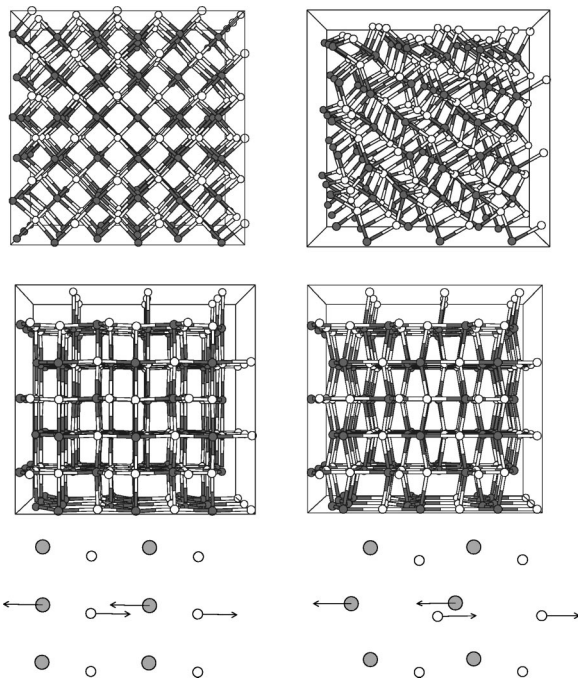


FIG. 3. The upper-left panel is ZB at 0 GPa, the upper-right panel is distorted structure at 39 GPa, the middle-left panel is *Cmcm* structure at 54 GPa, and the middle-right panel is *Imm2* at 57 GPa. In the upper and middle panels, the dark atoms are Ga and white ones are As. The lower-left panel is *Cmcm* and the right one is *Imm2* and in these panels Ga and As is not identified. The lower panels correspond to the simple picture of transition path.

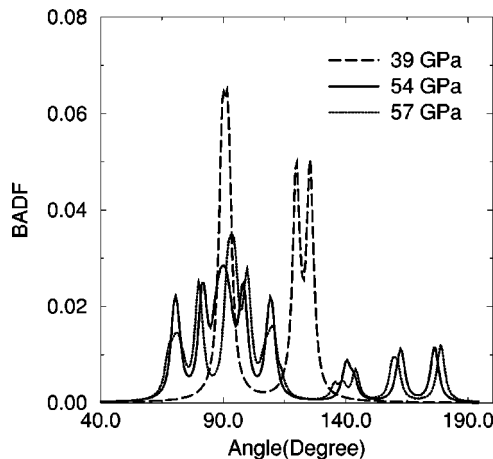


FIG. 2. The bond angle distribution function is calculated using a Gaussian representation and the width of broadening is $\sim 2^\circ$.

A gradual phase change to an orthorhombic structure for GaAs-III occurs at 57 GPa (Fig. 4). The structure, of space group *Imm2*, consists of a body-centered orthorhombic lattice with bases (0,0,0) and (0,1/2, Δ). This transition is in excellent agreement with the earlier experiment.¹ This structure, however, has not been seen in the recent experiment³ and hence there are some doubts about the identity of the GaAs-III phase. The present study suggests that there is a transition to *Imm2* phase.

The lattice parameters obtained for *Imm2* are $a = 4.63 \text{ \AA}$, $b = 4.55 \text{ \AA}$, and $c = 2.435 \text{ \AA}$, which are less than the experimental value of $a = 4.92 \text{ \AA}$, $b = 4.79 \text{ \AA}$, and $c = 2.635 \text{ \AA}$. The important parameter of *Imm2* is Δ that ranges between 0.25 and 0.5. When $\Delta = 0.25$ and $b/a = 1$, the symmetry increased and *Imm2* phase becomes β -Sn structure, and when $\Delta = 0.5$ the structure becomes *Immm*. In the case of $\Delta = 0.5$ and $b/c = \sqrt{3}$, *Imm2* turns to simple hexagonal structure. We find that $\Delta \sim 0.325$, which is slightly less than the experimental result of $\Delta = 0.425$ but lies on the range $0.25 < \Delta < 0.5$.

In order to elucidate the transition path, a simple picture is depicted in Fig. 3. The dark atoms belong to the first (001)

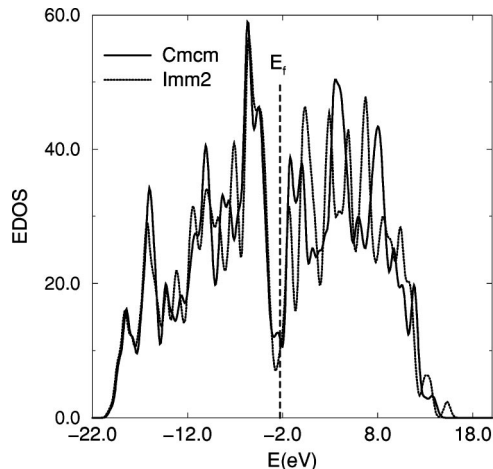


FIG. 4. EDOS of *Cmcm* at 54 GPa and *Imm2* at 57 GPa.

TABLE II. Structural parameters at zero temperature for ZB. Equilibrium volume per molecule V_0 , bulk modulus K , and pressure derivative of bulk modulus K' .

K (GPa)	K'	V_0 (\AA^3 per molecule)
74.19 ^a	4.6 ^a	44.812 ^a
74.0 ^b	4.6 ^b	44.135 ^b
75.0 ^c	4.49 ^c	45.168 ^d

^aPresent study.

^bReference 9 (theoretical).

^cReference 21 (experiment).

^dReference 22 (experiment).

plane and white ones to the second (001) plane in the lower panels of the figure. For clarity we do not identify Ga and As atoms, and the shift of the atoms is exaggerated. The atoms with arrow on the second (010) plane are most active in the transformation from $Cmcm$ to $Imm2$ and the arrows indicate the direction of displacement. The atoms on the second (010) and the first (001) planes move to $[\bar{1}00]$ direction whereas those on the second (010) and (001) planes move to $[100]$ direction. This opposite displacement leads to a transformation from $Cmcm$ to $Imm2$. With this transition path, it can be seen that a large displacement of the active atoms yields a transition to simple hexagonal structure. This picture also supports gradual transitions of $Cmcm \rightarrow Imm2 \rightarrow$ simple hexagonal.

B. Phase transitions from Gibbs free energy

The ZB, $Cmcm$ and $Imm2$ structures are optimized at several volumes using a constant-volume simulation. The total energy per molecule versus the volume is shown in Fig. 1. The energies at minimized structures are fit to the third-order Birch-Murnaghan equation of state;²⁰

$$E(V) = E_0 + \frac{9}{8} K V_0 [(V_0/V)^{2/3} - 1]^2 \times \left\{ 1 + \left(\frac{4 - K'}{2} \right) \left[1 - \left(\frac{V_0}{V} \right)^{2/3} \right] \right\}. \quad (1)$$

The equilibrium volume V_0 , the bulk modulus at zero temperature and pressure, K and its pressure derivative K' for the ZB phase are given in Table II. The calculated parameters for the ZB structure are in excellent agreement with the experimental and theoretical studies.

In the constant-volume simulation, we find that Δ parameter of $Imm2$ phases reaches the lower limit 0.25 (the smallest value for which $Imm2$ is defined) near 3 GPa and hence below this pressure $Imm2$ phase becomes unstable and transforms to a $Cmcm$ structure.

As found in the previous study of silicon¹⁵ and other simulations,^{10,11} the predicted transition pressure from Parrinello–Rahman simulations is much higher than experimental values. In order to obtain an equilibrium critical pressure, we calculate the Gibbs free energy ($G = E_{tot} + PV$) at zero temperature for ZB and $Cmcm$ and $Imm2$ structures. The Gibbs free-energy curve of ZB and $Cmcm$ phase (Fig.

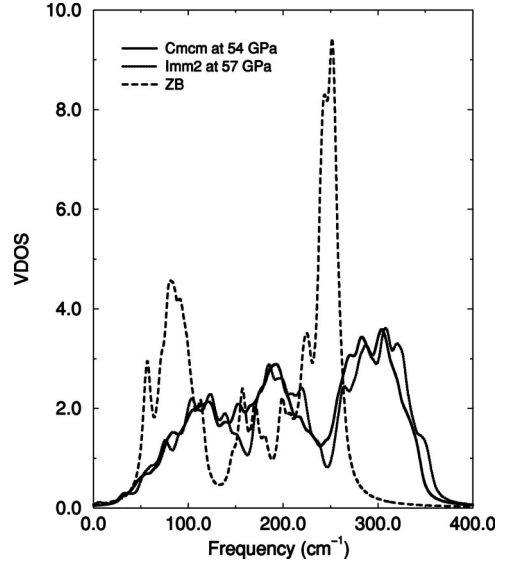


FIG. 5. VDOS of ZB structure at zero pressure, $Cmcm$ at 54 GPa, and $Imm2$ at 57 GPa.

1) crosses at about 23.5 GPa, indicating a first-order phase transition. Although the critical pressure is higher than the starting pressure of 17 GPa, it is close to the value of 22–23.4 GPa at which the transformation is completed. The transition from ZB to $Imm2$ occurs at 24 GPa, which is in excellent agreement with the experimental result of 24 GPa. The free energy of $Cmcm$ phase is lower than that of $Imm2$ up to 30 GPa, indicating that $Cmcm$ phase is more stable than $Imm2$. In the pressure range 30–55 GPa, the Gibbs free energy of both structures becomes equal and it is not well defined which structure is more stable. This is compatible with a continuous phase change between these structures.

It is also argued that the GaAs-II phase is a semiconductor or semimetal.¹ The electron density of states (EDOS) of the high-pressure phases is depicted in Fig. 4. We find that both high-pressure phases of GaAs are semimetals.

The vibrational density of states (VDOS) is depicted in Fig. 5. The optical and acoustic bands are broadened and their intensity decreases dramatically. The acoustic modes are softened while the optical modes shift into higher frequencies. The VDOS of $Cmcm$ phase can be separated into three bands; below 120 cm^{-1} , in the range of $120\text{--}240 \text{ cm}^{-1}$, and above 240 cm^{-1} . For $Imm2$ phase, these bands are well separated with a shift to high frequencies.

IV. CONCLUSIONS

We have studied the pressure-induced phase transition in GaAs with an *ab initio* constant-pressure relaxation. GaAs exhibits a first-order phase transition to $Cmcm$ structure at 54 GPa. With the increase of pressure a continuous phase change to $Imm2$ occurs at 57 GPa. The method identifies both high-pressure phases of GaAs with large values of metastable transition pressures. Nevertheless, the simulations provide detailed information about the pressure-induced phase transitions in GaAs. On the other hand, at the present thermodynamic criterion of the Gibbs free energies is required to estimate accurate transition pressures.

ACKNOWLEDGMENTS

We would like to thank Professor Jianjun Dong for many helpful discussions, and Dr. A. A. Demkov and Professor O.

F. Sankey for the Parrinello–Rahman method implementation in the FIREBALL96. This work was supported by the National Science Foundation under Grant Nos. DMR-00-81006 and DMR-00-74624.

-
- ¹S.T. Weir, Y.K. Vohra, C.A. Vanderborg, and A.L. Ruoff, Phys. Rev. B **39**, 1280 (1989).
²S.B. Zhang and M.L. Cohen, Phys. Rev. B **39**, 1450 (1989).
³M.I. McMahon and R.J. Nelmes, Phys. Status Solidi B **198**, 389 (1996).
⁴R.J. Nelmes, M.I. McMahon, N.G. Wright, and D.R. Allan, Phys. Rev. Lett. **73**, 1805 (1994).
⁵R.J. Nelmes and M.I. McMahon, Phys. Rev. Lett. **74**, 106 (1995).
⁶A. Mujica and R.J. Needs, J. Phys.: Condens. Matter **8**, L237 (1996).
⁷M.I. McMahon and R.J. Nelmes, Phys. Rev. Lett. **78**, 3697 (1997).
⁸A.A. Kelsey, G.J. Ackland, and S.J. Clark, Phys. Rev. B **57**, R2029 (1998).
⁹A. Mujica, A. Muñoz, and R.J. Needs, Phys. Rev. B **57**, 1344 (1998).
¹⁰K. Mizushima, S. Yip, and E. Kaxiras, Phys. Rev. B **50**, 14 952 (1994).
¹¹I.H. Lee, J.W. Jeong, and K.J. Chang, Phys. Rev. B **55**, 5689 (1997).
¹²M. Parrinello and A. Rahman, Phys. Rev. Lett. **45**, 1196 (1980).
¹³O.F. Sankey and D.J. Niklewski, Phys. Rev. B **40**, 3979 (1989).
¹⁴A.A. Demkov, O.F. Sankey, J. Gryko, and P.F. McMillan, Phys. Rev. B **55**, 6904 (1997).
¹⁵M. Durandurdu and D.A. Drabold, Phys. Rev. B **64**, 041201 (2001).
¹⁶M. Durandurdu and D.A. Drabold, Phys. Rev. B **65**, 104208 (2002).
¹⁷J.M. Besson, J.P. Itié, A. Polian, G. Weill, J.L. Mansot, and J. Gonzalez, Phys. Rev. B **44**, 4214 (1991).
¹⁸G.J. Ackland, Rep. Prog. Phys. **64**, 483 (2001).
¹⁹S.R. Phillpot, J.F. Lutsko, D. Wolf, and S. Yip, Phys. Rev. B **40**, 2831 (1989); J.F. Lutsko, D. Wolf, S.R. Phillpot, and S. Yip, *ibid.* **40**, 2841 (1989); S.R. Phillpot, S. Yip, and D. Wolf, Comput. Phys. **3**, 20 (1989).
²⁰F. Birch, J. Geophys. Res., [Atmos.] **91**, 4949 (1986).
²¹H.J. McSkirmin, A. Jayaraman, and P. Andreatch, Jr., J. Appl. Phys. **38**, 2362 (1967).
²²*Elastic, Piezoelectric, Piezooptic, and Electrooptic Constant of Crystals*, edited by O. Madelung, Landolt-Börnstein, New Series, Group III, Vol. 1 (Springer-Verlag, Berlin, 1966).